# A Study on Setting Half-life of Effective Rainfall as a Standard of Debris Flow Occurrence by Considering Geology

Naomasa HONDA[1*]

[1] Faculty of Regional Environment Science, Tokyo University of Agriculture
(1-1-1 Sakuragaoka, Setagaya-ku, Tokyo 1568512, Japan)
*Corresponding author. E-mail: nh205379@nodai.ac.jp

This study discusses how to set the half-life of effective rainfall as a standard of debris flow occurrence while also giving consideration to geological conditions. We investigated debris flow disasters at three different Japanese locations (the Osumi district, Nagiso town, and Hiroshima city) and calculated rainfall index *R'*, which expresses the rainfall history with a single value that combines long-term and short-term effective rainfalls. Our results suggest that around 20% of *R'* increases or decreases based on the differences in setting the half-life value by considering geology. However, we need to focus our attention on when the long-term half-life is less than 12 hours (e.g., with such volcanic ash as shirasu), since *R'* considerably decreases when it is calculated under those conditions. Geology greatly influences effective rainfall and *R'* as viewed through half-life. Consequently, precise prediction of debris flow occurrences is expected by incorporating geological feature information in calculating rain indexes.

**Key words:** effective rainfall, half-life, rainfall index *R'*, geology, debris flow occurrence

## 1. INTRODUCTION

Generally, both previous prolonged rainfall and the most recent episodic but strong rainfall affect debris flow occurrence [*Yano*, 1990; *Ushiyama et al.*, 2001]. When they act on the ground, which has such inherent factors as weak geological features and topography, and when resistance to sediment-related disasters exhausted, mass movements of material and sediment runoff begins [*Takahashi*, 1977; *Egashira et al.*, 1997]. Studies have been conducted on the relationships among geology, rainfall runoff characteristics, and sediment-related disasters, as well as on establishing rain indexes as warnings of sediment- related disasters [*Suzuki et al.*, 1978; *Kato et al.*, 2000; *Kurihara and Yamakoshi*, 2005; *Onda et al.*, 2006; *Nakai et al.*, 2007; *Honda et al.*, 2014; *Honda*, 2016].

Kurihara and Yamakoshi concentrated on the relationship between soil storage characteristics and debris flow occurrence, and they performed a runoff analysis using a tank model to determine the half-life of effective rainfall based on geological features [*Kurihara and Yamakoshi*, 2005]. Nakai et al. proposed rainfall index *R'*, which expresses rainfall history with a single value that combines long-term effective rainfall ($R_w$) and short-term effective rainfall ($r_w$) [*Nakai et al.*, 2007]. Honda et al. showed that both slope failure occurrence time and *R'* at that time were different for slopes in spite of studying adjacent slopes, and they assumed that this difference originated in the differences in geological features, topography, and covering vegetation [*Honda et al.*, 2014]. In addition, Honda showed that the precision of risk judgment of sediment-related disaster occurrences by *R′* might improve by considering geologic differences, based on previous results of examining debris flow [*Honda*, 2016].

In this study, our purpose is to develop a guideline of the setting half-lives of effective rainfall and rainfall index *R'* as a standard of debris flow occurrence, giving consideration to geology. We investigated debris flow disasters at three different Japanese locations: the Osumi district, Nagiso town, and Hiroshima city, all of which have specific rainfall conditions and geological features.

## 2. METHOD

### 2.1 Effective rainfall

Effective rainfall $R_t$ is a standard value used to investigate debris flow occurrences that applies the impact of past rainfall. It is calculated as follows [*Yano*, 1990]:

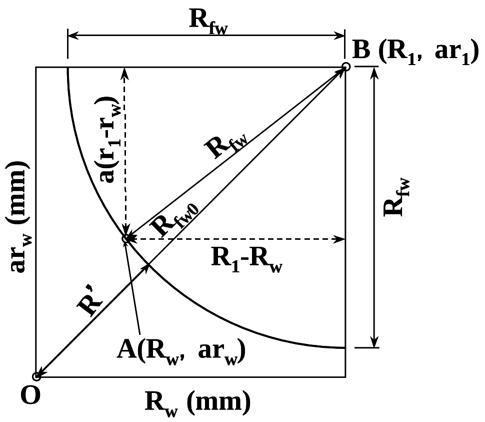


**Fig. 1** Rainfall index *R*'

$$R_t = r_t + \sum_{n=1}^{x} a_n r_{t-x} = r_t + a_1 r_{t-1} + \cdots + a_x r_{t-x} \tag{1}$$

$$a_n = 0.5^{n/T} \tag{2}$$

where $t$ is time, $r_t$ is precipitation, $a_n$ is the decrease coefficient, and $T$ is half-life. Generally, for $T$, the value of 1.5 hours and 72 hours used for short-term and long-term effective rainfall, respectively. In this study, short-term effective rainfall is denoted by $r_w$, while long-term effective rainfall is denoted by $R_w$.

### 2.2 Rainfall index *R'*

Rainfall index *R'* is calculated as follows [*Nakai et al.*, 2007]:

$$R_{fw} = \sqrt{(R_1 - R_w)^2 + a^2 (r_1 - r_w)^2} \tag{3}$$

$$R' = R_{fw0} - R_{fw} \tag{4}$$

where $R_{fw}$ is the long diameter of an oval, $R_1$ and $r_1$ are its central coordinates ($R_1 = ar_1$), $R_{fw0}$ is a value for $R_w = r_w = 0$, and $a$ is a coefficient to replace the oval with a circle (**Fig. 1**).

## 3. COMPUTATIONAL CONDITIONS

### 3.1 Outline of debris flows

In the Osumi district in Kagoshima Prefecture (**Fig. 2**), several debris flows were caused by the devastating typhoon No. 4 of July 2007. **Table 1** shows the debris flow occurrence time, the surface geology, and the gradient. **Figure 3** shows the observed rainfall data and the debris flow occurrence time at the nearest rainfall gauging station.


**Fig. 2** Locations of three actual basins

**Table 1** Debris flow occurrence in Osumi district

| No. | Occurrence Time | Rainfall gauging | Surface geology | Gradient (degrees) |
|---|---|---|---|---|
| [1] | 7/14 12:00 | Kihoku | Shirasu | 25～30 |
| [2] | 7/11 7:00 | Tashiro | Granite | 25～35 |
| [3] | 7/14 11:00 | Tashiro | Shirasu | 20～25 |
| [4a]※ | 7/4 0:00 | Sata | Shirasu | 20～30 |
| [4b]※ | 7/11 2:00 | Sata | Shirasu | 20～30 |
| [5] | 7/11 7:00 | Sata | Sandstone | 15～20 |
| [6] | 7/11 9:00 | Sata | Shale | 25～35 |

※ [4a] and [4b] are different debris flows on the same slope.

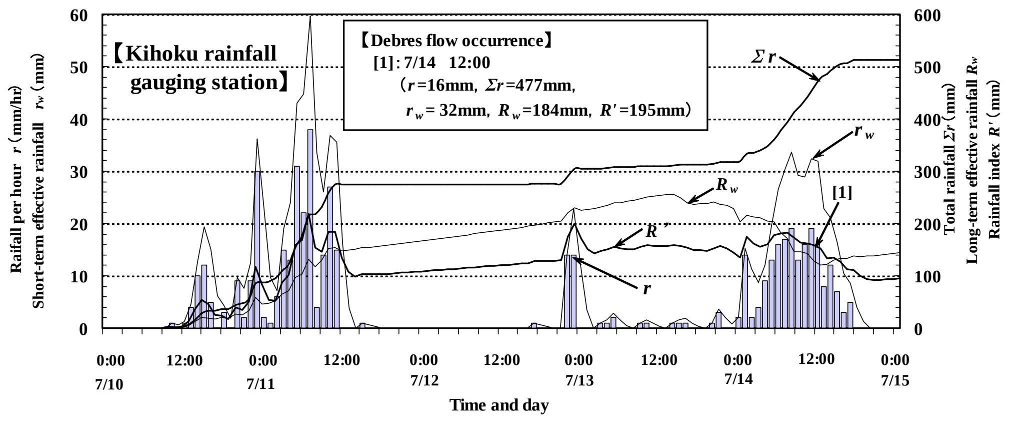


(a) Case of [1]

**Fig. 3** Relationship between observed rainfall and debris flow occurrence in the Osumi district
($a$ = 3, $R_1$ = 600 mm, and $r_1$ = 200 mm, which are necessary for calculating $R'$, as shown in section **3.2**)

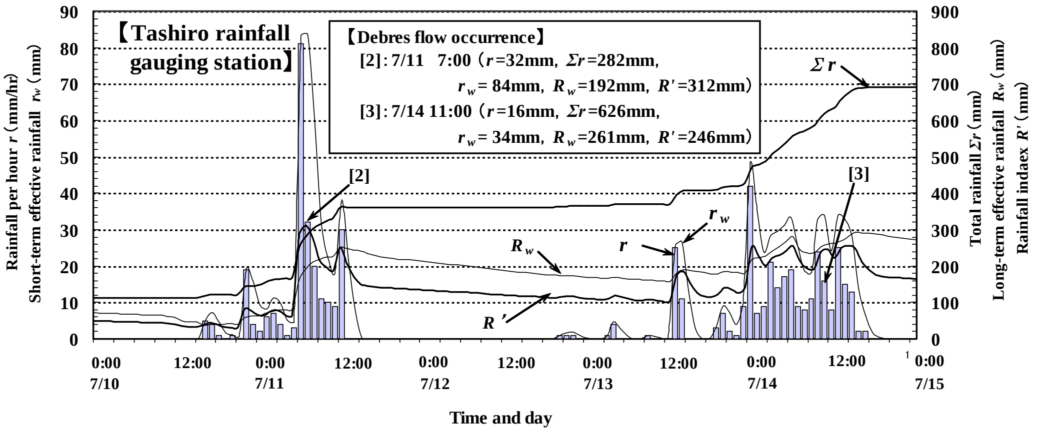


(b) Cases of [2] and [3]

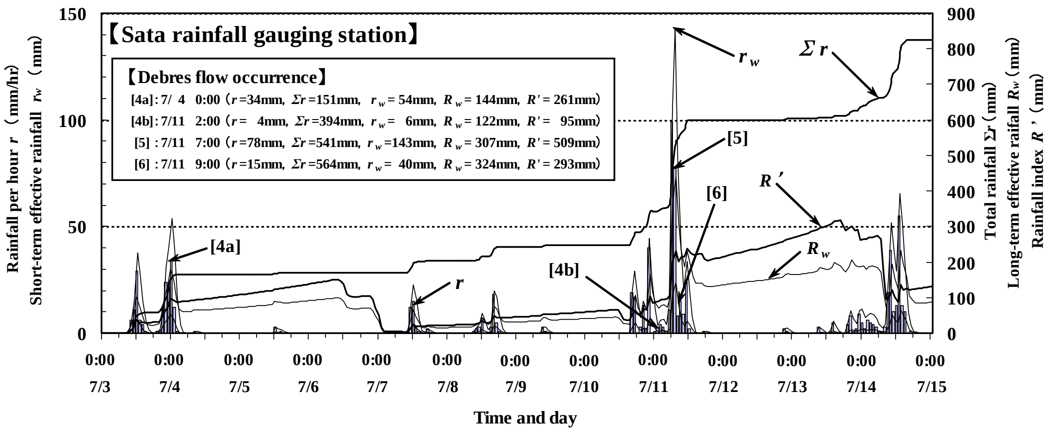


(c) Cases of [4a], [4b], [5], and [6]

**Fig.3** (continued) Relationship between observed rainfall and debris flow occurrence in the Osumi district ($a$ = 3, $R_1$ = 600 mm, and $r_1$ = 200 mm, which are necessary for calculating $R'$, as shown in section **3.2**)

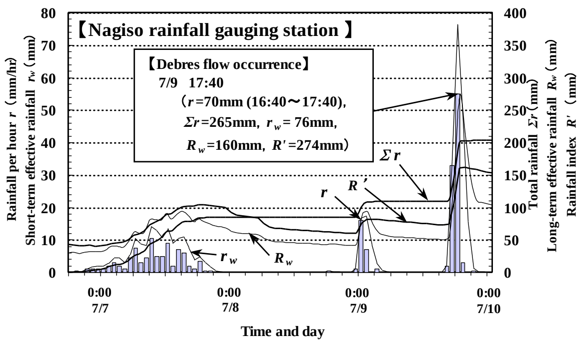


**Fig.4** Relationship between observed rainfall and debris flow occurrence in Nagiso town ($a$ = 3, $R_1$ = 600 mm, and $r_1$ =200 mm, as shown in section **3.2**)

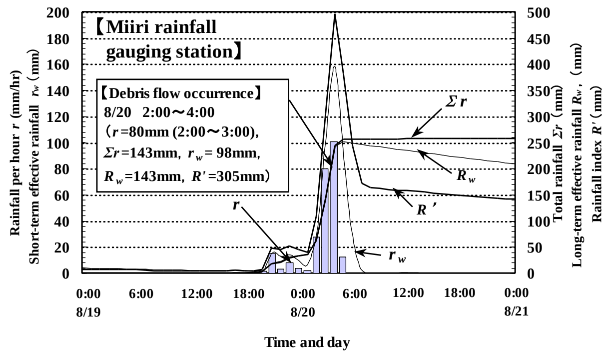


**Fig.5** Relationship between observed rainfall and debris flow occurrence in Hiroshima city ( $a$= 3, $R_1$ = 600 mm, and $r_1$ = 200 mm, as shown in section **3.2**)

In Nagiso town in Nagano Prefecture (**Fig. 2**), a debris flow was caused by heavy rainfall in July 2014. The surface geology of the debris flow occurrence zone was granite, and the gradient exceeded 30 degrees. **Figure 4** shows the observed rainfall data and the debris flow occurrence time at the nearest rainfall gauging station.

In Hiroshima city in Hiroshima Prefecture (**Fig. 2**), several debris flows were caused by heavy rainfall in August 2014. The surface geology of the debris flow occurrence zone was granite, and the gradient was about 20 degrees. **Figure 5** shows the observed rainfall data and the debris flow occurrence time at the nearest rainfall gauging station.

### 3.2 Computational conditions

$r_w$ and $R_w$ are calculated based on the observed rainfall data (**Figs. 3**, **4**, and **5**). Here, in reference to previous research (**Table 2**) [*Kurihara and Yamakoshi*, 2005], the condition of the short-term effective rainfall's half-life changed from 30 minutes to 2.0 hours, and the long-term effective rainfall's half-life changed from 3 to 72 hours.

$R_1$, $r_1$, and $a$ ($R_1 = ar_1$), are necessary for calculating $R'$, and we can select them in any combination. As a condition of the present study, $R_1$ should be decided by the value of $R_w$ (cross axis of the graph), which can express all of the calculation results on the same graph for comparison. According to the calculation results, we judged that 600 mm was an appropriate value for $R_1$.

$a$ is determined by the test calculations that produced $R_1$ while assuming $a$. In this study, $R_1$ is given with 600 mm and $a$ is assumed to be 3, 4 and 5. As a result, $a$ = 3 most closely matches all of the examples on the same graph. The preceding study also used $a$ = 3 [*Nakai et al.*, 2007]. Therefore, we adopted these values: $R_1$ = 600 mm, $a$ = 3, and $r_1 = R_1/a$ = 200 mm.

**Table 2** Half-life of effective rainfall for predicting debris flow occurrence according to geological features [*Kurihara and Yamakoshi*, 2005]

| Geology | Half-life (hr) | |
|---|---|---|
| | Short-term | Long-term |
| Granite | 1〜2 | 24〜48 |
| Sedimentary rock | 1〜2 | 12〜72 |
| Volcanic ashes | 1 or less | 12 or less |

## 4. RESULTS AND DISCUSSION

**Table 3** shows the calculation results of $r_w$, $R_w$, and $R'$ for long-term $T$=12 hr, 24 hr, 48 hr, and 72 hr. **Figure 6** shows the relationships among $r_w$, $R_w$, $R'$, and $T$ by geological features.

In **Fig. 6**, the subscripts of each sign, for example, $R'_{72,\ 1.5}$, are the half-lives used for the calculation. In the vertical axis of **Fig. 6**, no dimensions by values were calculated using general-purpose half-lives (short-term $T$ = 1.5 hours and long-term $T$ = 72 hours), i.e., $r_{w1.5}$, $R_{w72}$, and $R'_{72,\,1.5}$.

### 4.1 Relationships among *T*, $r_w$, and $R_w$

#### 4.1.1 Relationship between *T* and $r_w$

As shown in **Table 3**, **Figs. 6(a)(1)**, **(b)(1)**, and **(c)(1)**, when short-term $T$ ranges from 1.0 to 2.0 hours, $r_{wT}/r_{w1.5}$ ranges from 0.72 to 1.17, except for $r_{w1.0}/r_{w1.5}$ and $r_{w2.0}/r_{w1.5}$ of Sata [6] (**Table 3,** $r_{w1.0}/r_{w1.5}$ = 0.48 and $r_{w2.0}/r_{w1.5}$ = 1.50).

In Sata [6] (**Fig. 3(c)**), a brief but strong rainfall of 78 mm per hour fell 2.0 hours before a debris flow. These rainfall data did not influence $r_{w1.0}$, while on the other hand they strongly affected $r_{w.2.0}$.

According to **Table 2**, short-term $T$ of the volcanic ash is less than 1.0 hour. As shown in **Table 3** and **Fig. 6(a)(1)** (for volcanic ash), when short-term $T$ equals 30 minutes, $r_{w0.5}/r_{w1.5}$ ranges from 0.65 to 0.83. Furthermore, when short-term $T$ equals 1.0 hour, $r_{w1.0}/r_{w1.5}$ ranges from 0.72 to 0.83, except for Sata [4b] (**Table 3**, $r_{w1.0}/r_{w1.5}$ = 1.00). These values are considerably smaller than 1.00 (for general- purpose short-term $T$ = 1.5 hours).

Sata [4a] and [4b] have different debris flows on the same slope (identical inherent factors). Since Sata [4b] occurred several days after Sata [4a] (**Table 1** and **Fig. 3(c)**), Sata [4b] might have an occurrence mechanism unlike the others.

#### 4.1.2 Relationship between *T* and $R_w$

As shown in **Table 3**, **Figs. 6(a)(1)**, **(b)(1)**, and **(c)(1)**, when long-term $T$ ranges from 24 to 72 hours, $R_{wT}/R_{w72}$ ranges from 0.70 to 1.00, except for Nagiso town (**Table 3**, $R_{w24}/R_{w72}$ = 0.65 and $R_{w48}/R_{w72}$ = 0.69). In Nagiso town, even though a large amount of rain fell three days before the debris flow occurrence (**Fig. 4**), these rainfall data did not influence Nagiso' s $R_{w24}$ and $R_{w48}$.

According to **Table 2**, long-term $T$ of the volcanic ash is less than 12 hours. As shown in **Table 3** and **Fig. 6(a)(1)** (for volcanic ash), when long-term $T$ equals 12 hours, $R_{w12}/R_{w72}$ ranges from 0.56 to 0.74, which is considerably smaller than 1.00 (for general-purpose long-term $T$ = 72 hours).

According to **Table 2**, long-term $T$ of the accretionary complexes ranges from 12 hours to 72 hours. As shown in **Table 3** and **Fig. 6(a)(1)** (for accretionary complexes), when long-term $T$ equals 12 hours, $R_{w12}/R_{w72}$ ranges from 0.66 to 0.73. These results are considerably smaller than 1.00 (for general-purpose long-term $T$ = 72 hours).

#### 4.1.3 Considerations

According to our results, when $r_w$ and $R_w$ are calculated using $T$ in consideration of geology, an increase or decrease of about 20% to 30% occurs in comparison with the results by the general-purpose values of $T$, except for volcanic ash.

In general, areas with volcanic ash deposits have a low tendency to be penetrated, and both the long-term and short-term half-lives are very small [*Kurihara and Yamakoshi*, 2005]. Moreover, when $R'$ is calculated by these short half-lives rather than by the generally used value of T, it drops by more than 30%. Similarly, for accretionary complexes, $R'$ considerably also decreases when the long-term half-life is less than 12 hours. We must carefully set the half-lives for such geology as volcanic ash and accretionary complexes, and our

**Table 3** Examples of calculation results

| Long-term $T$ (hr) | Rainfall (mm) | Volcanic ashes (Shirasu) | | | | | | | | | | | | | | | |
|---|---|---|---|---|---|---|---|---|---|---|---|---|---|---|---|---|---|
| | | Kihoku [1] | | | | Tashiro [3] | | | | Sata [4a] | | | | Sata [4b] | | | |
| | | Short-term $T$ (hr) | | | | Short-term $T$ (hr) | | | | Short-term $T$ (hr) | | | | Short-term $T$ (hr) | | | |
| | | 0.5 | 1.0 | **1.5** | 2.0 | 0.5 | 1.0 | **1.5** | 2.0 | 0.5 | 1.0 | **1.5** | 2.0 | 0.5 | 1.0 | **1.5** | 2.0 |
| | $\boldsymbol{r_w}$ | 21 | 23 | **32** | 37 | 22 | 28 | **34** | 38 | 40 | 45 | **54** | 62 | 5 | 6 | **6** | 7 |
| | $r_w/r_{w\,1.5}$ | 0.66 | 0.72 | **1.00** | 1.16 | 0.65 | 0.82 | **1.00** | 1.12 | 0.74 | 0.83 | **1.00** | 1.15 | 0.83 | 1.00 | **1.00** | 1.17 |
| 12 | $R_w$ | 125 | | | | 147 | | | | 107 | | | | 73 | | | |
| | $R_w/R_{w\,72}$ | 0.68 | | | | 0.56 | | | | 0.74 | | | | 0.60 | | | |
| | $R'$ | 130 | 141 | 156 | 167 | 148 | 162 | 175 | 185 | 160 | 171 | 189 | 204 | 61 | 62 | 64 | 65 |
| | $R'/R'_{72,\,1.5}$ | 0.67 | 0.72 | 0.80 | 0.86 | 0.60 | 0.66 | 0.71 | 0.75 | 0.74 | 0.79 | 0.88 | 0.94 | 0.64 | 0.65 | 0.67 | 0.68 |
| 24 | $R_w$ | 145 | | | | 201 | | | | 131 | | | | 86 | | | |
| | $R_w/R_{w\,72}$ | 0.79 | | | | 0.77 | | | | 0.91 | | | | 0.70 | | | |
| | $R'$ | 144 | 155 | 169 | 181 | 182 | 196 | 210 | 221 | 176 | 188 | 206 | 222 | 69 | 71 | 72 | 73 |
| | $R'/R'_{72,\,1.5}$ | 0.74 | 0.79 | 0.87 | 0.93 | 0.74 | 0.80 | 0.85 | 0.90 | 0.81 | 0.87 | 0.95 | 1.03 | 0.73 | 0.75 | 0.76 | 0.77 |
| 48 | $R_w$ | 176 | | | | 231 | | | | 140 | | | | 96 | | | |
| | $R_w/R_{w\,72}$ | 0.96 | | | | 0.89 | | | | 0.97 | | | | 0.79 | | | |
| | $R'$ | 164 | 175 | 190 | 202 | 199 | 214 | 228 | 239 | 183 | 195 | 213 | 229 | 77 | 77 | 79 | 80 |
| | $R'/R'_{72,\,1.5}$ | 0.84 | 0.90 | 0.97 | 1.04 | 0.81 | 0.87 | 0.93 | 0.97 | 0.85 | 0.90 | 0.99 | 1.06 | 0.81 | 0.81 | 0.83 | 0.84 |
| **72** | $\boldsymbol{R_w}$ | **184** | | | | **261** | | | | **144** | | | | **122** | | | |
| | $R_w/R_{w\,72}$ | **1.00** | | | | **1.00** | | | | **1.00** | | | | **1.00** | | | |
| | $\boldsymbol{R'}$ | 169 | 180 | **195** | 208 | 216 | 231 | **246** | 257 | 185 | 197 | **216** | 231 | 92 | 94 | **95** | 97 |
| | $R'/R'_{72,\,1.5}$ | 0.87 | 0.92 | **1.00** | 1.07 | 0.88 | 0.94 | **1.00** | 1.04 | 0.86 | 0.91 | **1.00** | 1.07 | 0.97 | 0.99 | **1.00** | 1.02 |

| Long-term $T$ (hr) | Rainfall (mm) | Accretionary complexes | | | | | | | | Granite | | | | | | | | | | | |
|---|---|---|---|---|---|---|---|---|---|---|---|---|---|---|---|---|---|---|---|---|---|
| | | Sata [5] | | | | Sata [6] | | | | Tashiro [2] | | | | Nagiso | | | | Hiroshima | | | |
| | | Short-term $T$ (hr) | | | | Short-term $T$ (hr) | | | | Short-term $T$ (hr) | | | | Short-term $T$ (hr) | | | | Short-term $T$ (hr) | | | |
| | | 0.5 | 1.0 | **1.5** | 2.0 | 0.5 | 1.0 | **1.5** | 2.0 | 0.5 | 1.0 | **1.5** | 2.0 | 0.5 | 1.0 | **1.5** | 2.0 | 0.5 | 1.0 | **1.5** | 2.0 |
| | $r_w$ | 103 | 128 | **143** | 154 | 17 | 19 | **40** | 60 | 52 | 73 | **84** | 91 | 63 | 72 | **76** | 79 | 87 | 94 | **98** | 101 |
| | $r_w/r_{w\,1.5}$ | 0.72 | 0.90 | **1.00** | 1.08 | 0.43 | 0.48 | **1.00** | 1.50 | 0.62 | 0.87 | **1.00** | 1.08 | 0.83 | 0.95 | **1.00** | 1.04 | 0.89 | 0.96 | **1.00** | 1.03 |
| 12 | $R_w$ | 224 | | | | 214 | | | | 140 | | | | 88 | | | | 133 | | | |
| | $R_w/R_{w\,72}$ | 0.73 | | | | 0.66 | | | | 0.73 | | | | 0.55 | | | | 0.93 | | | |
| | $R'$ | 372 | 414 | 435 | 447 | 178 | 182 | 232 | 277 | 210 | 251 | 272 | 284 | 195 | 211 | 221 | 227 | 267 | 289 | 297 | 303 |
| | $R'/R'_{72,\,1.5}$ | 0.73 | 0.81 | 0.85 | 0.88 | 0.61 | 0.62 | 0.79 | 0.95 | 0.67 | 0.80 | 0.87 | 0.91 | 0.71 | 0.77 | 0.81 | 0.83 | 0.88 | 0.95 | 0.97 | 0.99 |
| 24 | $R_w$ | 263 | | | | 271 | | | | 156 | | | | 104 | | | | 138 | | | |
| | $R_w/R_{w\,72}$ | 0.86 | | | | 0.84 | | | | 0.81 | | | | 0.65 | | | | 0.97 | | | |
| | $R'$ | 402 | 447 | 470 | 483 | 208 | 213 | 265 | 314 | 221 | 262 | 284 | 297 | 207 | 223 | 233 | 239 | 279 | 293 | 301 | 306 |
| | $R'/R'_{72,\,1.5}$ | 0.79 | 0.88 | 0.92 | 0.95 | 0.71 | 0.73 | 0.90 | 1.07 | 0.71 | 0.84 | 0.91 | 0.95 | 0.76 | 0.81 | 0.85 | 0.87 | 0.91 | 0.96 | 0.99 | 1.00 |
| 48 | $R_w$ | 279 | | | | 294 | | | | 165 | | | | 111 | | | | 140 | | | |
| | $R_w/R_{w\,72}$ | 0.91 | | | | 0.91 | | | | 0.86 | | | | 0.69 | | | | 0.98 | | | |
| | $R'$ | 415 | 461 | 485 | 499 | 220 | 225 | 278 | 328 | 228 | 269 | 291 | 304 | 212 | 229 | 238 | 244 | 281 | 295 | 303 | 308 |
| | $R'/R'_{72,\,1.5}$ | 0.82 | 0.91 | 0.95 | 0.98 | 0.75 | 0.77 | 0.95 | 1.12 | 0.73 | 0.86 | 0.93 | 0.97 | 0.77 | 0.84 | 0.87 | 0.89 | 0.92 | 0.97 | 0.99 | 1.01 |
| **72** | $\boldsymbol{R_w}$ | **307** | | | | **324** | | | | **192** | | | | **160** | | | | **143** | | | |
| | $R_w/R_{w\,72}$ | **1.00** | | | | **1.00** | | | | **1.00** | | | | **1.00** | | | | **1.00** | | | |
| | $\boldsymbol{R'}$ | 435 | 483 | **509** | 524 | 234 | 239 | **293** | 344 | 246 | 290 | **312** | 326 | 247 | 264 | **274** | 280 | 283 | 297 | **305** | 310 |
| | $R'/R'_{72,\,1.5}$ | 0.85 | 0.95 | **1.00** | 1.03 | 0.80 | 0.82 | **1.00** | 1.17 | 0.79 | 0.93 | **1.00** | 1.04 | 0.90 | 0.96 | **1.00** | 1.02 | 0.93 | 0.97 | **1.00** | 1.02 |

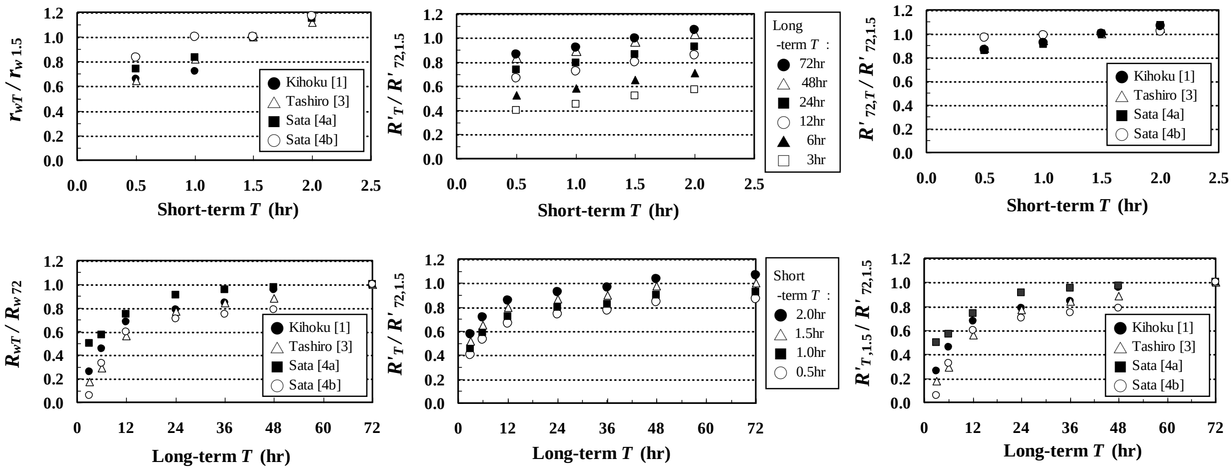


(1) Relationships among $T$, $r_w$ and $R_w$

(2) Examples of relationship between $T$ and $R'$ (Kihoku [1])

(3) Relationship between $R'_{72,\,1.5}$ and $R'_{T,\,1.5}$ ($T$ : long-term half-life)

(a) Case of volcanic ash (Shirasu)

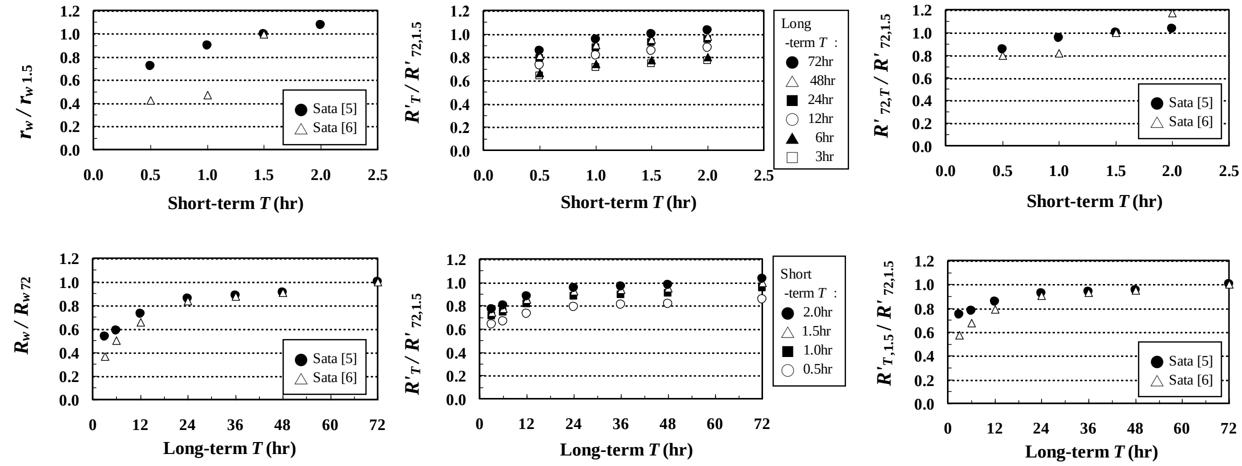


(1) Relationships among $T$, $r_w$ and $R_w$

(2) Examples of relationship between $T$ and $R'$ (Sata [5])

(3) Relationship between $R'_{72,\,1.5}$ and $R'_{T,\,1.5}$ ($T$: long-term half-life)

(b) Case of accretionary complexes (sandstone and shale)

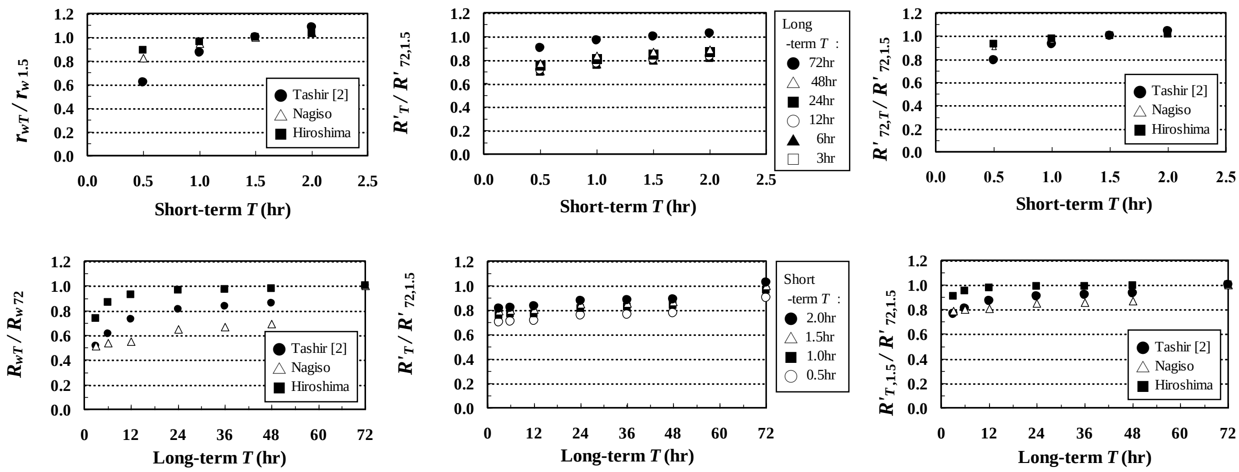


(1) Relationships among $T$, $r_w$ and $R_w$

(2) Examples of relationship between $T$ and $R'$ (Nagiso)

(3) Relationship between $R'_{72,\,1.5}$ and $R'_{T,\,1.5}$ ($T$: long-term half-life)

(c) Case of granite

**Fig.6** Relationships among $R_w$, $r_w$, $R'$, and $T$ corresponding to geology purpose is to develop a guideline of the setting half-lives of effective rainfall while considering geology, although attention must also be given to rainfall conditions before a debris flow occurrence, i.e., episodic but strong rainfall as well as total amount of rainfall.

### 4.2 Relationships among *T*, *R′*, and geology

#### 4.2.1 Relationship between *T* and *R′*

As shown in **Figs. 6(a)(2)**, **(b)(2)**, and **(c)(2)**, when long-term *T* is constant and short-term *T* ranges from 30 minutes to 2.0 hours, the fluctuation range of $R'_T/R'_{72,\ 1.5}$ with a change in short-term *T* is almost always less than 20%. Similarly, when short-term *T* is constant and long-term *T* ranges from 12 hours to 72 hours, the fluctuation range of $R'_T/R'_{72,1.5}$ with a change in long-term *T* almost always reaches below 20%. These results are slightly smaller than the fluctuation ranges of $r_w$ and $R_w$ with the change in *T* (increase or decrease from about 20% to 30%, Section **4.1.3**), since *R′* expresses the rainfall history by a single value that combines $r_w$ and $R_w$.

#### 4.2.2 Relationships among *T*, *R′*, and geology

When we focus our attention on the fluctuation range of $R'_T/R'_{72,\ 1.5}$ with a change in long-term *T*, the increase rate of $R'_T/R'_{72,\ 1.5}$ becomes small where *T* = 12 hours is a boundary in **Figs. 6(a)(2)** and **(b)(2)**, i.e., for volcanic ash and accretionary complexes. On the other hand, it is nearly constant in **Fig. 6(c)(2)**, i.e., for granite. Even though volcanic ash and accretionary complexes are not uniform for the rainfall runoff characteristics and the half-life, granite has uniformity [*Kurihara and Yamakoshi*, 2005]. Thus, we assume that the non-homogeneity of the half-life due to geological characteristics influences effective rainfalls and *R'*.

**Figures 6(a)(3)**, **(b)(3)**, and **(c)(3)** show examples of $R'_{72,\ T}/R'_{72,\ 1.5}$ with a change in short- term *T* for long-term *T* = 72 hours and $R'_{T,\ 1.5}/R'_{72,\ 1.5}$ with a change in long-term *T* for short-term *T* = 1.5 hours.

When long-term *T* equals 72 hours, the fluctuation range of $R'_{72,\ T}/R'_{72,\ 1.5}$ with a change in short-term *T* is almost always less than 20%. When short-term *T* equals 1.5 hours, the fluctuation range of $R'_{T,\ 1.5}/R'_{72,\ 1.5}$ with a change in long-term *T* in the range from 12 to 72 hours almost always reaches below 20%, except for **Fig. 6(a)(3)**, i.e., for volcanic ash. In addition, when long-term *T* ranges from 24 to 72 hours, the fluctuation range of $R'_{T,\ 1.5}/R'_{72,\ 1.5}$ with a change in long-term *T* is almost always less than 20%, except for Sata [4b] in **Fig. 6(a)(3)** (**Table 3,** $R'_{24,\ 1.5}/R'_{72,\ 1.5} = 0.76$). The uniqueness of Sata [4b] was mentioned above (section **4.1.1**).

When we focus our attention on the fluctuation range of $R'_{T,\ 1.5}/R'_{72,\ 1.5}$ with a change in long-term *T*, the increase rate of $R'_{T,\ 1.5}/R'_{72,\ 1.5}$ becomes small where *T*=12 is a boundary in **Figs. 6(a)(3)** and **(b)(3)**, i.e., for volcanic ash and accretionary complexes. On the other hand, the fluctuation range is nearly constant in **Fig. 6(c)(3)**, i.e., for granite. They have the same tendency in the case of $R'_T/R'_{72,\ 1.5}$ (**Figs. 6(a)(2)**, **(b)(2)**, and **(c)(2)**). Even though volcanic ash and accretionary complexes are not uniform for the rainfall runoff characteristics and the half-life, granite has uniformity [*Kurihara and Yamakoshi*, 2005]. Thus, we assume that the non-homogeneity of the half-life due to geological characteristics influences effective rainfalls and *R'*.

#### 4.2.3 Considerations

According to the results, when *R′* is calculated using *T* in consideration of geology, an increase or decrease of less than 20% occurs in comparison with the results by the general-purpose values of *T*. However, we excluded the cases where the geological features are comprised of volcanic ash or accretionary complexes and long-term *T* is 12 hours or less. This is our intention when we consider the geological elements of *R′*.

### 4.3 Example of *R′* for investigating the application range of *T*

Judging from the previous work's results [**4.1**, **4.2**], we assume that short-term *T* in practice ranges from 1.0 to 2.0 hours and long-term *T* ranges from 24 to 72 hours. **Figure 7** shows the relationship between the effective rainfalls of the debris flow occurrence and *R'* curves. The combinations of *T* used for calculation are short-term *T* = 1.0 hour and long-term *T* = 24 hours (none " ' " plots in **Fig. 7**), and short-term *T* = 2.0 hours and long-term *T* = 72 hours (available " ' " plots in **Fig. 7**).

In **Table 3**, the combinations of none " ' " and available " ' " plots in **Fig. 7** range from 0.77 to 1.17 (the increase or decrease is mostly less than 20%) except for Sata [6] ($R'/R'_{72,\ 1.5} = 0.73$) and Sata [4b] ($R'/R'_{72,\ 1.5} = 0.75$). The uniqueness of Sata [6] and Sata[4b] was mentioned above (section **4.1.1**).

In the Osumi district, much of the debris flow occurred in the distribution of such volcanic sediment as shirasu (**Table 1,** Kihoku[1], Tashiro[3], Sata[4a], and Sata[4b]), which is generally not too hard and poor against water. Each *R'* value at the time of a debris flow occurrence was small (**Fig. 7**). Such flow occurrences also occurred in an incline area that ranged from 20 to 30 degrees (**Table 1**).

Spots also exist where each *R'* value at the time of debris flow occurrences was large (**Fig. 7**).

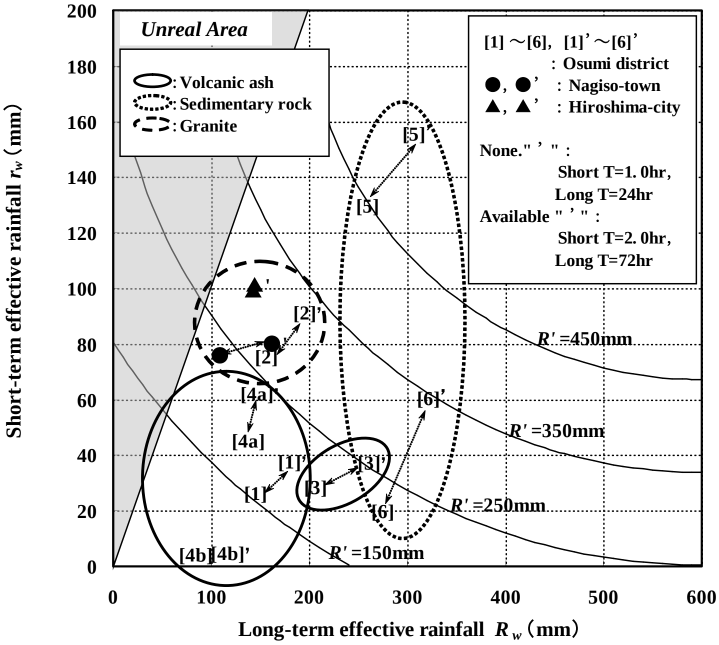


**Fig. 7** Relationship between effective rainfalls of debris flow occurrence and curves of *R'*

Their geological features are granite (**Table 1**, Tashiro [2] in the Osumi district, Nagiso town, and Hiroshima city) and sedimentary rock of such accretionary complexes as sandstone and shale (**Table 1**, Sata [5] and Sata [6]). They are harder than volcanic sediment.

For such similar geological features as Sata [5] and Sata [6], *R'* of the latter at the time of debris flow occurrences is smaller than that of the former, and this difference in *R'* is large. This is because the incline of Sata [6] is steep, and it is a weak point for sediment-related disasters.

**Figure 7**, which considers the application range of *T*, shows a very useful guideline as a standard of debris flow occurrence by *R'*.

## 5. CONCLUSIONS

This study discussed an approach to establishing the half-life of effective rainfall as a standard of debris flow occurrence. Although we focused our attention on only nine spots, we derived the following conclusions:

(1) When $r_w$ and $R_w$ are calculated using *T* based on geological features, an increase or decrease of about 20% to 30% occurs in comparison with the results obtained by the general-purpose values of *T* (short-term $T$ = 1.5 hours and long-term $T$ = 72 hours), except for such volcanic ash as shirasu.

(2) When *R'* is calculated using *T* based on geological features, an increase or decrease of less than 20% occurs in comparison with the results by the general-purpose values of *T*; however, we excluded the results when the geological features are volcanic ash or accretionary complexes and long-term *T* is 12 hours or less.

(3) (1) and (2) allow us to derive a useful guideline when we investigate the geological composition in relation to *R'*, although we must also give attention to the rain conditions before debris flow occurrences, i.e., episodic but strong rainfall and total amount of rainfall. Furthermore, care is required when the long-term half-life is less than 12 hours.

(4) When the calculation result of *R'*, which considers the application range of *T*, is shown with the *R'* curves, it is a very useful guideline as a standard of debris flow occurrence.

(5) Geology greatly influences effective rainfall and *R'* through half-lives. We expect to precisely predict debris flow occurrences by adding geological feature information to rain indexes.

**ACKNOWLEDGMENT:** Part of this study was supported by the Strategic Research Project of Tokyo University of Agriculture.

### REFERENCES

Egashira, S., Miyamoto, K. and Itoh, T. (1997): Bed-lopd Rate in View of Two Phase Flow Dynamics. Annuals of Hydraulic Engineers, Japan Society of Civil Engineering, Vol.41, pp.789-797 (in Japanese with English abstract).

Honda, N., Kato, N. and Kasai, M. (2014): Relationship between surface failure due to rainfall and geology - Experience of sediment-related disasters in Miyazaki Prefecture due to typhoon No. 4 and No.5 in July 2007 as example -. Journal of the Japan Society of Erosion Control Engineering, Vol. 66(6), pp. 25-30 (in Japanese with English abstract).

Honda, N. (2016): A Study on Relationship among Rainfall, Geology Characteristics and Debris Flow Occurrence. Annuals of Hydraulic Engineers, Japan Society of Civil Engineering, Vol.60, pp.241-246 (in Japanese with English abstract).

Kato, Y., Onda, Y., Mizuyama, T., Kosugi, K., Yoshikawa, I., Tsujimura, M., Hata, K. and Okamoto, M. (2000): The Difference of Runoff Peak Response Time in Upstream of Ibi River Underlain of Different Geology. Journal of the Japan Society of Erosion Control Engineering, Vol. 53(4), pp. 38–43 (in Japanese with English abstract).

Kurihara, J. and Yamakoshi, T. (2005): Study on Effective Rainfall for Prediction of Debris Flow Occurrence Base on Rainfall Runoff Characteristics. Outline of Priority Research Projects Report, Public Works Research Institute, pp.629-634 (in Japanese).

Nakai, S., Kaibori, M., Sasaki, Y. and Moriwaki, T. (2007): Applicability of a New Rainfall Index R' for Recent Cases and Proposal of the Method for Warning against Sediment-related Disaster. Journal of the Japan Society of Erosion Control Engineering, Vol. 60(1), pp. 37–42 (in Japanese with English abstract).

Onda, Y., Tsujimura, M., Tanaka, T., Sasaki, K., Mizuyama, T., Uchida, T., Tainaka, O. and Tanaka, H. (2006): Determining the Criteria Rainfall for Debris Flow Warning and Evacuation by Rainfall-Runoff response. Journal of the Japan Society of Erosion Control Engineering, Vol. 58(5), pp. 13–17 (in Japanese).

Suzuki, M., Fukushima, Y., Takei, A. and Kobashi, S. (1978): The Critical Rainfall for the Disasters Caused by Debris Movement. Journal of the Japan Society of Erosion Control Engineering, Vol. 31(3), pp. 1–7 (in Japanese with English abstract).

Takahashi, T. (1977): A Mechanism of Occurrence of Mud-Debris Flow and their Characteristics in Motion. Annuals of Disaster Prevention Research Institute, Kyoto University, Vol. 20B-2, pp. 405–435 (in Japanese with English abstract).

Ushiyama, M., Ohido, S. and Takara, K (2001): The Critical Line for Sediment Disaster Warning Based on Precipitation Data in Hiroshima Prefecture in June 1999. Advances in River Engineering, Japan Society of Civil Engineering, Vol.7, pp.167-170 (in Japanese with English abstract).

Yano, K. (1990): Study of the Method for Setting Standard Rainfall of Debris Flow by the Reform of Antecedent Rain. Journal of the Japan Society of Erosion Control Engineering, Vol. 43(4), pp. 3-13 (in Japanese with English abstract).